Annals of Nuclear Energy 37 (2010) 1014–1025

Contents lists available at ScienceDirect

Annals of Nuclear Energy

journal homepage: www.elsevier.com/locate/anucene

Technical note

Simulation of a gas-cooled fluidized bed nuclear reactor – Part II: Stability of a fluidized bed reactor with mixed oxide fuels

B.E. Miles *, C.C. Pain, J.L.M.A. Gomes

Department of Earth Sciences and Engineering, Imperial College, London, UK

ARTICLE INFO

Article history:
Received 23 October 2009
Received in revised form 14 March 2010
Accepted 16 March 2010

Keywords:
Fluidized bed reactor
Coupled Radiation Transport Multiphase Fluid Dynamics
FETCH
Transient
Plutonium

ABSTRACT

Fertile materials can be converted by nuclear reaction into a transuranic mixture with a fissile content, mostly plutonium isotopes. Fuel which includes a limited proportion of plutonium is already used in some reactors. Use is restricted by the smaller delayed neutron yield and lower negative temperature coefficient of reactivity compared with uranium fuels.

A reactor with an additional stability feedback would make possible an increased use of plutonium fuels. This feedback mechanism is present in a novel conceptual High Temperature Gas Cooled Reactor (HTGR) where the TRISO particles are fluidized by the coolant gas.

Spatial and time dependent simulations using the coupled Radiation Transport and Computational Multiphase Fluid Dynamic code FETCH are applied to investigations of this stability. The reactor has been investigated using plutonium fuel of various isotopic compositions. The temperature coefficient of reactivity may not be negative, depending on the isotopic composition of the fuel. The reactor is found stable. The amplitudes of power fluctuations increase however. These cause fluctuations in fuel temperature which can be excessive unless the average power is reduced, compared with that produced from a uranium fuel.

The time dependent calculations are repeated using, in the neutron transport, data representing hypothetical fuels with zero temperature coefficient and/or zero delayed neutron yield.

1. Introduction

1.1. Background

The predicted increase in the consumption of electrical energy will require increased use of nuclear energy. At the same time concerns over the disposal of radio-active waste require an environmentally responsible fuel cycle. A logical way to achieve this is a greater utilisation of fissile material converted from fertile material. The conversion process is known as breeding.

^{235}U is the sole fissile isotope which occurs naturally. Natural uranium contains only 0.7% of this isotope. Because of neutron capture the majority of currently operating reactors require 3–5% fissile uranium (Low Enriched Uranium, LEU). In a preceding paper (Miles et al., submitted for publication), firstly the nuclear properties of fuels containing the bred material were compared with those of LEU. Secondly the types of reactor which can use the converted fissile material were compared.

In the 1960s and 1970s there was considerable interest in the breeding of fissile material (see, for example Glasstone, 1967). Some developments in the commercial energy market in the last few years make it once again worthwhile to consider the conversion of fertile material to fissile. An increased price of enriched uranium is an incentive to convert the fertile ^{238}U in depleted uranium to fissile plutonium. Depleted uranium then becomes an asset rather than a cost.

In reprocessing plants, such as Sellafield and Cap la Hague, spent fuel from power reactors is separated by means of chemical processes into uranium, plutonium (approximately 1% of the total) and fission products. There is also a stock of plutonium containing more than 90% fissile isotopes, referred to in the literature as Weapons Grade plutonium (WG) (Stacey, 2004).

An example of fissile plutonium recycle is the mixed uranium and plutonium oxide fuel (MOX) already used to a limited extent in some Light Water Reactors (NEA/OECD, 2006). Some safety restraints are described in Galperin (1995). They are related to reactivity feedback, control rod worth, boron worth, moderator temperature coefficient (MTC) and shutdown margin (see Franceschini and Petrovic, 2008).

An international benchmarking exercise certifies codes for the utilisation of WG plutonium in MOX. A basis for benchmark analyses (Thilagam et al., 2009) is 1/3 MOX in a typical 1000 MW electrical VVER PWR. The European Utility Requirements (EUR) document states that the next generation of European reactor core design shall be optimised for UO_2 fuel assemblies with provision

* Corresponding author.
E-mail address: bryan.miles01@imperial.ac.uk (B.E. Miles).

0306-4549/$ - see front matter © 2010 Elsevier Ltd. All rights reserved.
doi:10.1016/j.anucene.2010.03.009

Nomenclature

$\mathbf{x}$	(vector) point in space	T_s	temperature of a particle surface (K)
T	reactor response time (s)	T_g	temperature of the gas surrounding a particle (K)
k	neutron multiplication factor	q	typical steady fission power in a particle (W)
l	prompt neutron lifetime (s)	d_s	diameter of a particle (m)
h_{gs}	convective heat transfer coefficient, solid to gas ($W\,m^{-2}\,K^{-1}$)	C_{ps}	specific heat of the material in a particle ($J\,kg^{-1}\,K^{-1}$)
Re	Reynolds number	β	delayed neutron yield
Pr	Prandtl number	ρ_s	density of a particle ($kg\,m^{-3}$)
Nu	Nusselt number		

for up to 50% MOX assemblies. In Fetterman (2009) it is demonstrated that the Westinghouse AP1000 is capable of complying with this provision without significant design changes. The plutonium is from LWR spent fuel and the uranium in this MOX is tails material. The plutonium content in MOX varies from 9% to 17%. In Cuevas Vivas et al. (2002) a method is presented for optimising the distribution of a range of plutonium contents in MOX fuel elements. Here WG plutonium is used in PWR fuel and ex LWR plutonium in BWR fuel. Alternatives to uranium in MOX, neutronically inert oxides such as zirconia and alumina, are investigated in Lombardi and Mazzola (1996) and Paratte and Chawla (1995). Several studies describe possible changes to the design and operation of reactors, together with the processing of spent fuels, to reduce the volume of the long-life radio-toxicity of the waste by a factor of 100. The residual radioactivity left would then be comparable with that of the initial natural uranium after several hundred years (Frois, 2008).

The International Reactor Innovative and Secure (IRIS) is a small (1000 MW thermal) advanced Westinghouse Pressurised Water Reactor (PWR). An alternative fuel is a 100% MOX core (Franceschini and Petrovic, 2008). Its fissile content (^{239}Pu and ^{241}Pu) is 5.5% compared with 4.95% ^{235}U. Compared with a typical PWR the ratio of moderator (water) to fuel is increased by 50% because of safety restraints. An alternative method of increasing the moderator to fuel ratio in a PWR, by adding graphite in the centre of fuel rods, is described in Jo et al. (2000).

Modifications to the NEA/OECD benchmark fuel in a Boiling Water Reactor (BWR) are proposed in Francois et al. (2002). The moderator to fuel ratio is increased. The fuel is 100% MOX.

Several studies of the incineration of plutonium and Minor Actinides (MA) in HTGR are reported in Kuijper et al. (2006). The objective was maximum plutonium incineration. The fuel was pure plutonium oxide. About 70% of the plutonium was fissile (that indicates probable ex LWR plutonium). In these analyses high burnup in an HTGR compared with that in an LWR is found possible. For first generation fuel they are in the range of 70 MWd/kg for once-through fuel. They are very much higher, 700 MWd/kg, when the HTGR is a Pebble Bed Reactor (PBR) in which the fuel can be continuously recycled. Less than 20% of the plutonium remains in the finally discharged fuel. Temperature coefficients of reactivity remain negative. However, for a plutonium of a second generation the burn up has to be reduced, to about 440 MWd/kg with more than 40% of the plutonium remaining. Processing of HTGR spent fuel is described in Masson et al. (2006). After crushing and incineration of the PBR or block graphite in a matrix surrounding the TRISO particle, the particles themselves are fragmented and their kernels are dissolved in nitric acid.

Studies (Hoggett-Jones et al., 2002; Alander et al., 2006; Salvatores, 2006) compare reactor and accelerator approaches to spent nuclear fuel management.

Following conversion from fertile material, plutonium together with other transuranic elements can in principle be repeatedly separated from the fission products in spent fuel and recycled. The isotopic composition of these mixtures of transuranic elements, in particular the fissile content, depends on the neutron energy spectra in the reactors from which the fuels were recovered.

1.2. Objectives and review

A thermal reactor which can use more fissile transuranic isotopes would help to make better use of an energy resource and to reduce the radioactivity in nuclear waste.

A reactor which uses helium as a medium to fluidise a bed of particles and as a coolant to remove fission heat has been proposed (Rots and van der Hagen, 1996). The fuel is contained in 1 mm diameter coated particles consisting of a kernel of uranium or plutonium oxide with a diameter of 0.2–0.3 mm surrounded by several layers of graphite and silicon carbide. They are known as TRISO particles (TRistructural ISOtropic).

Stability of a nuclear reactor with respect to short term fluctuations of power level depends on reactivity variation with temperature. For different MOX fuels, the temperature coefficients of reactivity and their importance were discussed in a previous paper (Miles et al., submitted for publication). Depending on fuel composition, for example as fission products accumulate with burn up, and on the proportion of fuel and moderator in a pebble, it is possible for a coefficient to occur which is no longer negative.

Time dependent analyses of the fluidized bed reactor are presented in this paper for fuels in which hypothetical properties are simulated, including a zero temperature coefficient. Their behaviour is discussed and conclusions are drawn, in particular the fuels' ability to produce power. Zero delayed neutron fractions in fuels are also simulated. A feedback mechanism is identified which is important for stability of the reactor and which results from an interaction between neutronics and fluid mechanics.

2. Codes

Transient behaviour is analysed using the same deterministic time-dependant code FETCH as used in Miles et al. (submitted for publication).

Material neutron cross sections for use in FETCH are generated using the lattice cell code WIMS9A. Cross sections are self shielded and collision probabilities (Duderstadt and Hamilton, 1976; Stacey, 2004) are calculated. A data base for the material regions is condensed into six energy groups. The process is repeated at several temperature levels. The variation of the effective neutron multiplication factor k_{eff} with temperature is one of the feedback mechanisms which determine the time dependent stability of the reactor. As the temperature coefficient becomes less negative, stability has to be achieved by other means. To test whether this is possible, in a hypothetical fuel, WIMS data is modified so that the group constants produced at each temperature are identical. The time dependent behaviour of a fuel is also influenced by the

proportion of the fission neutrons which are not prompt but are delayed. In order to investigate the influence of the fraction of fission neutrons which are produced after a delay, a fuel with the hypothetical property of a zero fraction of such neutrons is specified in FETCH input files.

These two material properties are vital for the stability of conventional reactors which have fuels fixed in space. The results of tests in which these properties have been removed from the fuel and other materials in this reactor are presented and discussed in Section 3.

3. Time dependent calculations

3.1. Stability

In MOX fuel, ^{239}Pu has a lower delayed neutron yield (β) than ^{241}Pu. MOX fuel with WG plutonium has the largest ^{239}Pu content. This fuel is used as basis for hypothetical fuels in which the different feedback effects are investigated after having been isolated from each other. The conventional stability feedback mechanisms are removed, one by one.

The reactor which is used for this investigation is one already used in Miles et al. (submitted for publication). The introduction of a graphite cylinder into the centre of the fluidized bed was found to improve neutron economy. This variation in geometry (Fig. 1) is chosen for this investigation.

Firstly, the temperature coefficient of reactivity is set to zero. This coefficient would in reality be influenced during the operation of a reactor by the production of fission products. The fresh fuel has a negative temperature coefficient at all temperatures. Fission products can have the effect of making the coefficient more positive, at least at lower temperatures. A fuel with a zero coefficient could therefore have some practical significance. Secondly, the fuel has its delayed neutron yield set to zero. Even though this yield in MOX fuel with WG plutonium would already be small, setting it to zero is found to have an effect. Thirdly, both of these effects are set to zero, to see whether a reactor would become completely unstable.

Fig. 2 shows the variation of fission rate in a reactor with MOX WG plutonium fuel and zero temperature coefficient. In this logarithmic presentation the amplitude of the fission power oscillations can be seen. The average fission rate in time over the duration of the calculation is 4.6×10^{18} s^{-1} (equivalent to 147 MW thermal power), compared with 7.4×10^{18} s^{-1} (equivalent to 237 MW thermal power) from the normal fuel. The fluctuations in power and temperature are greater than those from MOX WG fuel with the normal temperature coefficient. Also the mean fission rate is less. The temperature difference can be seen more clearly in a comparison of the temperatures in Fig. 3. This shows that the fluctuations in spatial maximum temperature in the fuel with zero temperature coefficient are greater than those in normal MOX WG fuel. This, in turn, has greater fluctuations than those in LEU, showing the effect of the reduced temperature coefficient in the MOX fuel. The spatial maximum temperature (solid or coolant gas) is an indication of the coolant exit temperature and therefore of reactor power. The time dependent maximum temperature peaks over the duration of the calculation are also greater. A reactor with this

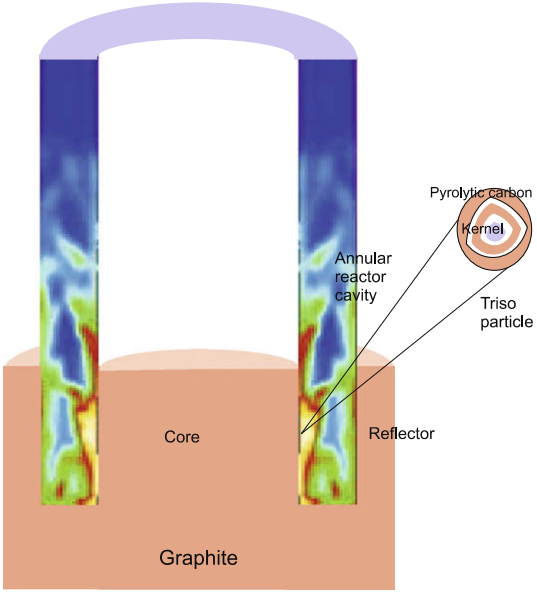

Fig. 1. Fluidized bed reactor schematic, showing an annular cavity between an inside graphite core and an outside reflector. The cavity contains a bed of fluidized TRISO particles. One of the particles is shown magnified and cut away to display the kernel and outer layers. The radius of the central graphite core is 2.5 m. The outer radius of the fuel bed is 3.5 m. The outer radius of the reflector is 4.5 m. The bottom reflector is 2 m thick. The side reflector extends to 5 m above the floor of the bed. The total height of the reactor is 15 m.

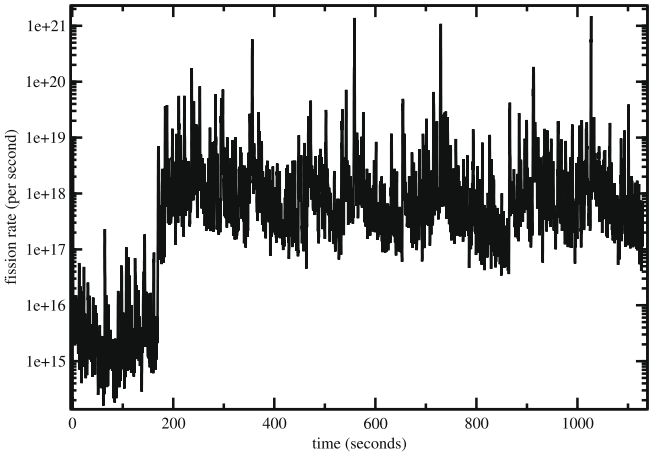

Fig. 2. Fluidized bed reactor with 8% recycled WG plutonium 92% depleted uranium, with hypothetical zero temperature coefficient – time dependent fission power.

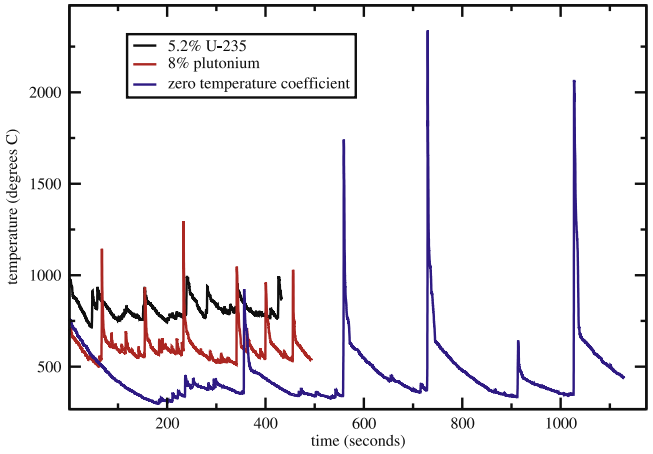

Fig. 3. Fluidized bed reactor with 8% recycled WG plutonium 92% depleted uranium (also hypothetical zero temperature coefficient) and with LEU – time and space dependent maximum temperature. The higher peak temperatures resulting resulting from less negative coefficients of reactivity can be seen.

hypothetical fuel is less stable than one with the real MOX fuel even though the time averaged power is less. Stability could be improved by changes in reflector and core geometry, resulting however in a further reduction in power. Such geometry changes increase neutron leakage at the greatest bed expansions. Compared with Fig. 2, the linear presentation (Fig. 4) shows more clearly the peaks in fission rate. Fig. 4 shows fission pulses, approximately at intervals of 200 s. The greatest pulse (1.58×10^{21} fissions/s, 50,000 MW) is at 1027.1 s. A more typical fission pulse, Fig. 5, occurs at 558.9 s. It is used as one of the examples to be analysed in detail when attempting to quantify the feedback mechanism when reactivity is reduced by dispersal of the fuel particles by heating and expansion of the intervening coolant gas (Fig. 6). Results from a hypothetical fuel with zero yield of delayed neutrons are compared in Fig. 7. A typical fission pulse with this fuel, Fig. 8, occurring at 264.2 s is also used as one of the examples to be analysed.

A less typical succession of peaks of the reactor fission rate, Fig. 9, resulting in the largest peak of temperature in this calculation, Fig. 10, occurs at 729.6 s. The time delay between peak fission power and peak temperature is in all of these examples 0.3 s. The convective heat transfer model in FETCH is such that the time dif-

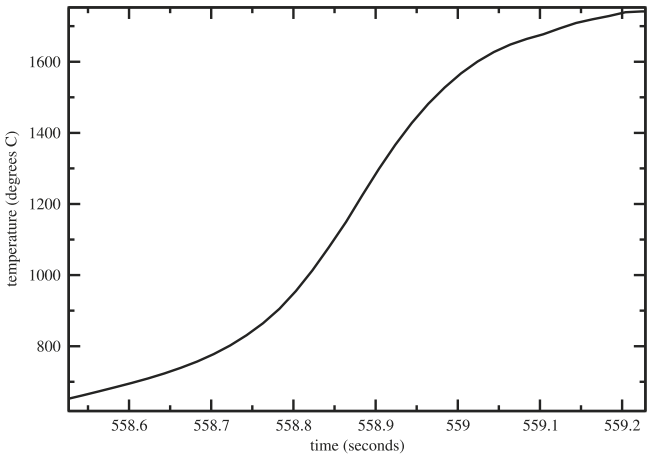

Fig. 6. Fluidized bed reactor with 8% recycled WG plutonium 92% depleted uranium, with hypothetical zero temperature coefficient – a peak temperature at 559.2 s.

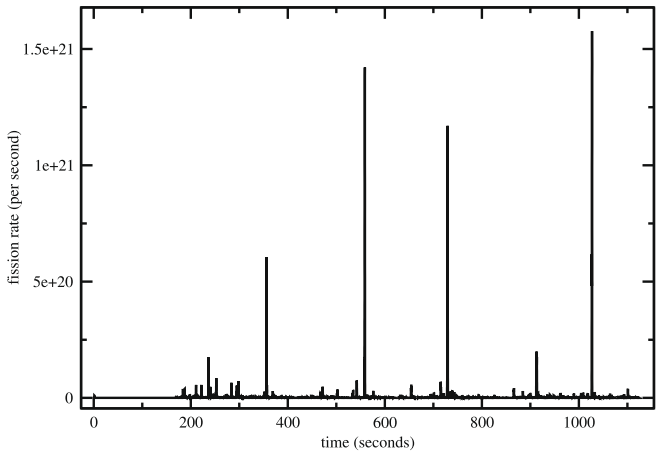

Fig. 4. Fluidized bed reactor with 8% recycled WG plutonium 92% depleted uranium, with hypothetical zero temperature coefficient – peak fission power trend with time.

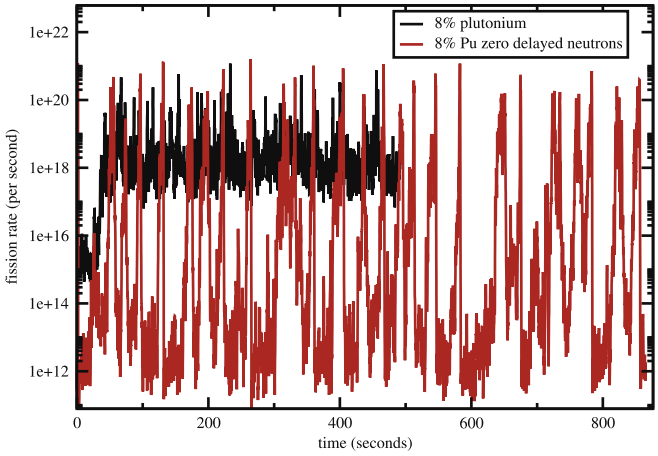

Fig. 7. Fluidized bed reactor with 8% recycled WG plutonium 92% depleted uranium, comparison with hypothetical zero delayed neutron yield.

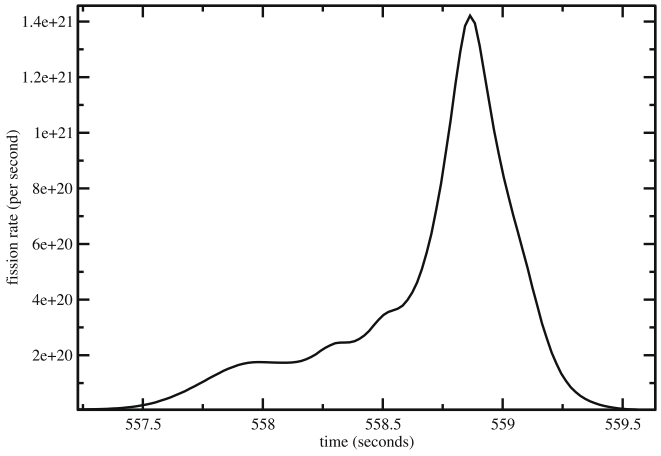

Fig. 5. Fluidized bed reactor with 8% recycled WG plutonium 92% depleted uranium, with hypothetical zero temperature coefficient – a typical peak fission power, at 558.9 s.

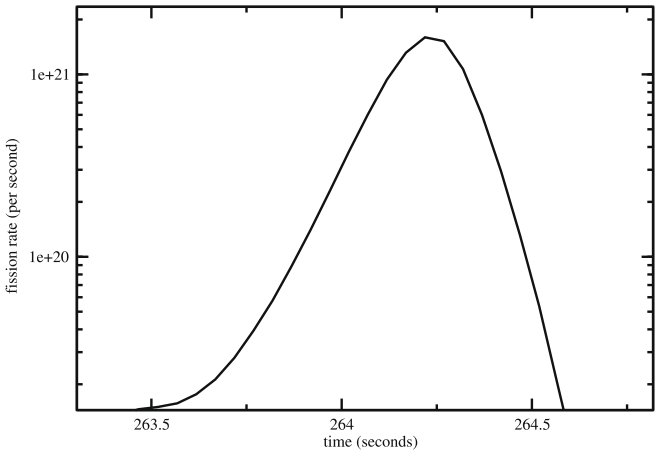

Fig. 8. Fluidized bed reactor with 8% recycled WG plutonium 92% depleted uranium, with hypothetical zero delayed neutron yield – a typical peak fission power, at 264.2 s.

ference between a peak in solid phase temperature and the corresponding peak in gas phase temperature is less than 0.05 s. Heat transfer around a particle is discussed in Section 3.2, based on calculations which make use of the constitutive equations as used in FETCH.

The successive pulses can be seen in both the reactor fission power and in the local fission rate indicated by the concentration of the short half life delayed neutron precursors at four locations on the reactor cavity walls (Fig. 11). These are at 0.6, 1 m and 1.4 m above the reactor fuel cavity floor on the inner (core) wall and at 1m on the outer (reflector) wall, locations where the local fission rate appears greatest.

The effect of the delayed fraction of fission neutrons on the stability of the reactor is investigated by setting the delayed neutron fraction to zero in what otherwise is normal MOX fuel with WG plutonium. The reactivity temperature coefficient is normal for this fuel. Fig. 7 compares the fission rates in normal MOX WG fuel and in the same fuel with zero delayed neutron yield. The greater fluctuations in initial fission rate and subsequent fission peaks from the hypothetical fuel are clear. The peak fission rates, even on the logarithmic scale, appear greater. The average fission rate over the duration of the calculation is approximately the same.

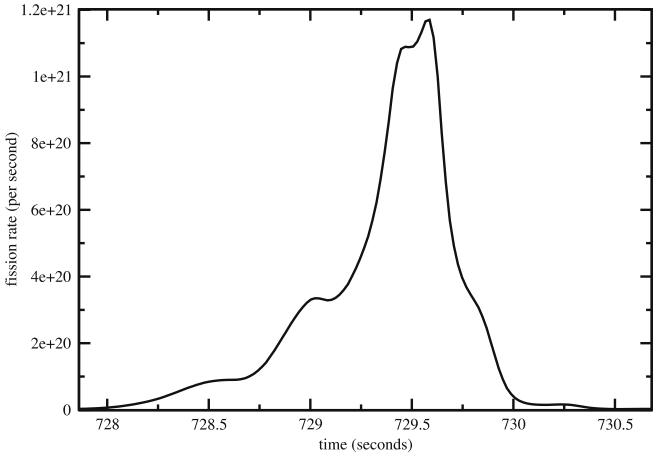

Fig. 9. Fluidized bed reactor with 8% recycled WG plutonium 92% depleted uranium, with hypothetical zero temperature coefficient – fission peak development showing smaller peaks building up to a maximum at 729.6 s.

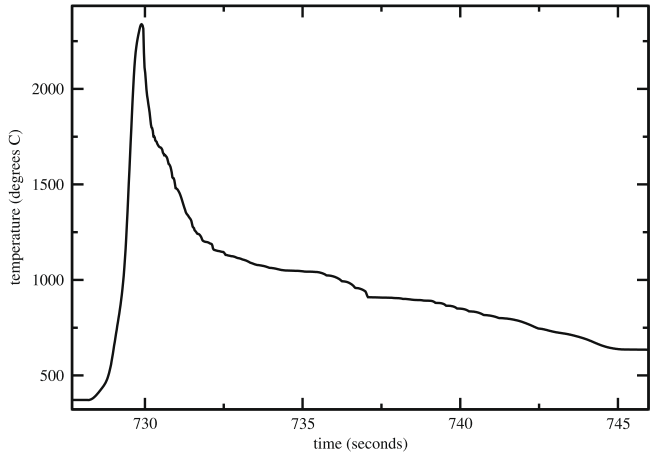

Fig. 10. Fluidized bed reactor with 8% recycled WG plutonium 92% depleted uranium, with hypothetical zero temperature coefficient – temperature peak development at 729.9 s.

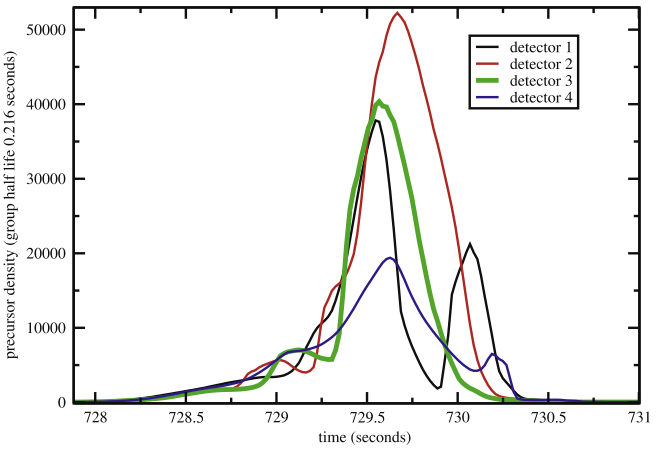

Fig. 11. Fluidized bed reactor with 8% recycled WG plutonium 92% depleted uranium, with hypothetical zero temperature coefficient. The delayed neutron precursors with the shortest half life are an indication of fission reaction density around 730 s at four detection locations. These are at 0.6 m, 1 m, 1.4 m above the fuel cavity floor on the inner wall, at 1 m on the outer wall.

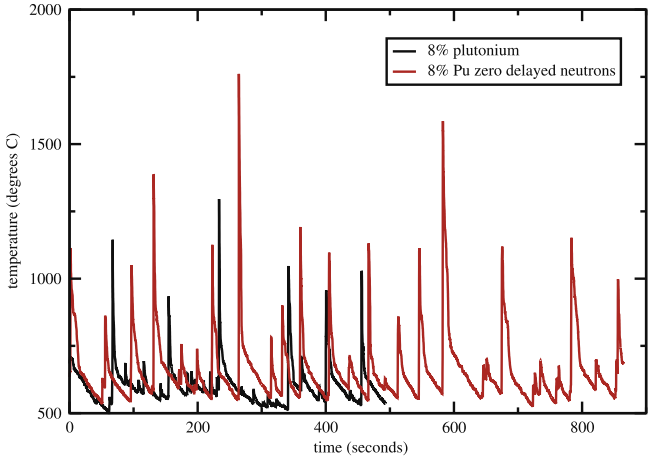

Fig. 12. Fluidized bed reactor with 8% recycled WG plutonium 92% depleted uranium, comparison with hypothetical zero delayed neutron yield.

Maximum temperatures are compared in Fig. 12. Peak temperatures occur at intervals which have a mean period of about 40 s, becoming longer after 600 s. The peak temperatures exceed those in the normal fuel. The greatest peak is lower than that which occurs when the temperature coefficient of reactivity is zero although the instantaneous peak fission powers are approximately equal. The stability worsens up to 270 s, then improves.

Finally both temperature coefficient and delayed neutron yield are set to zero. Again, when compared with the normal MOX WG fuel, the greater fluctuations in fission rate from the hypothetical fuel are clear (Fig. 13). The average fission rate over the duration of the calculation remains approximately the same as that of the normal fuel. However the greatest peak temperature is much higher than that which occurs with either of the other hypothetical fuels (Fig. 14). The stability worsens up to 520 s, then improves, with a period of 100 s.

In the cases shown in Figs. 12 and 14, where the temperature initially exceeds the target, when the stability has improved the temperature appears eventually to stay below the target value. The development of temperature with time in the fuel with zero temperature coefficient dose show increasing peaks in temperature up to 729.9 s, possibly downwards thereafter. Calculation over

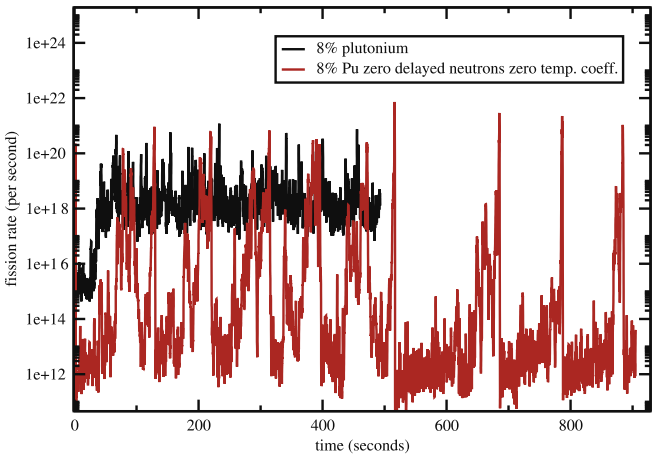

Fig. 13. Fluidized bed reactor with 8% recycled WG plutonium 92% depleted uranium, comparison with hypothetical zero delayed neutron yield and zero delayed neutrons – time dependent fission power.

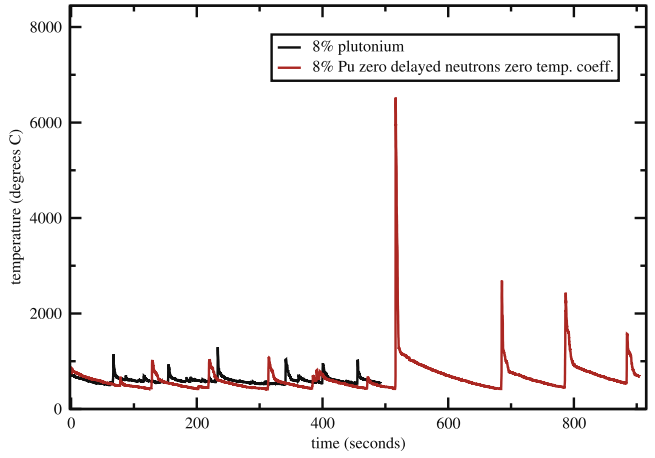

Fig. 14. Fluidized bed reactor with 8% recycled WG plutonium 92% depleted uranium, comparison with hypothetical zero delayed neutron yield and zero delayed neutrons – time dependent temperature. The greater temperature peaks can be seen.

a longer time would show whether the downward trends in peak values would continue.

3.2. Heat transfer in and around a particle

The heat transfer inside a particle and from particle to gas during the typical peak of fission rate, such as shown in Figs. 5 and 8, can be analysed in a simplified model. At the same time the rate of increase of fission rate can be related to the response of the reactor as predicted by the "Inhour" equation. These are in fuels with zero temperature coefficient of reactivity (Fig. 5) and zero delayed neutron yield (Fig. 8) respectively. The response time of the heat input from fission in the approach to both peaks is about 0.1 s. The fission rate response of the reactor is determined by the neutron lifetime divided by the surplus reactivity. When the surplus reactivity is less than the delayed neutron yield the effective neutron lifetime includes this delay and becomes therefore long. The reactor response is then slow, a time constant of several seconds.

The prompt neutron lifetime is 1×10^{-6} s in the fuel bed, based on the macroscopic absorption cross section and neutron velocities in the two highest energy groups as calculated by WIMS for EVENT and FETCH. This compares with 1×10^{-5} s in the reflector. Duderstadt and Hamilton (1976, Fig. 6-3) includes, for various neutron lifetimes, graphs of response time against surplus reactivity in fuel where ^{239}Pu is the fissile isotope. A response time of 1×10^{-1} s in such a fuel would imply a surplus reactivity of one dollar. In a hypothetical fuel with zero delayed neutron yield, Eq. (3-28) in Hetrick (1993) for a fast response with large reactivity, comes to resemble Eq. (6-47) in Duderstadt and Hamilton (1976), for a superprompt-critical step positive reactivity insertion.

$$T = \frac{l}{k-1} \tag{1}$$

The surplus reactivity is $k-1$. The period of the response T of the reactor is the solution to the "Inhour" equation when it ignores delayed neutrons. It would be, when $\beta = 0$ and $l = 1 \times 10^{-6}$ s, 1×10^{-1} s for a positive step reactivity of 1×10^{-5}. The response time in these numerical analyses is not determined by the reactivity of a uniformly arranged fuel. The spatial distribution of particles, the fast neutron leakage, the resonance escape probability and the thermal utilization in the fuel bed are not uniform. The response time is determined by the movement of particles, possibly adjacent to a bubble. This dispersal is discussed in Section 3.3.

An instantaneous reciprocal period of fission power is given in Fig. 10a of Pain et al. (2003). This has a maximum of 35 s^{-1} at start up, thereafter about 10 s^{-1} or less.

A steady nominal reactor power is typically 375 MW. There are 4.4×10^{10} particles in a reactor. The steady fission heat q per particle is 0.0085 W. The heat transfer from a particle to the gas phase is defined in a constitutive relation, the convective heat transfer equation in Table 3 of Pain et al. (2002). For an isolated TRISO particle as defined in Miles et al. (submitted for publication), the coefficient is

$$h_{gs} = 5400 \text{ W m}^{-2} \text{ K}^{-1}$$

and the non-dimensional groups

$$Re = 188, \quad Pr = 0.64, \quad Nu = 25$$

The particle diameter d_s is 1.03×10^{-3} m. The temperature difference $T_s - T_g$ between the particle surface and gas in these steady conditions is

$$T_s - T_g = q/\left(\pi d_s^2 h_{gs}\right) = 0.47\ ^\circ C \tag{2}$$

A step change from zero to a fission heat rate, a factor n compared with the steady average power per TRISO kernel, would lead to rate of temperature rise

$$dx/dt = ax + b$$

where $x = T_g - T_s$, $a = 6h_{gs}/(C_{ps}\rho_s d_s)$ and $b = 6nq/\left(C_{ps}\rho_s \pi d_s^3\right)$. C_{ps}, the particle heat capacity, is 1400 J kg^{-1} K^{-1} and ρ_s, the particle density, is 2060 kg m^{-3} (Miles et al., submitted for publication).

$$x = \frac{b}{a}(1 - e^{-at}) \tag{3}$$

$$T_s - T_g = 0.47n(1 - e^{-t/t_s})\ ^\circ\text{C} \tag{4}$$

where

$$t_s = 1/a = (C_{ps}\rho_s d_s)/6h_{gs} = 0.092 \text{ s}$$

The gas temperature T_g is assumed constant. T_s is the surface temperature of the particle. This will be same as the TRISO shell temperature, since the difference between the temperature of the outside surface of the kernel and T_s is small compared with $T_s - T_g$. After a step change a steady value of $T_s - T_g$ is re-established in a fraction of a second. The gas surrounding the particle is heated rapidly locally and expands.

The fission rate is assumed uniform within the kernel. The temperature difference between the centre of the kernel and its surface

in the steady heat flow 0.0085 W is 1.64 °C. The corresponding fission rate of the reactor is 1.2×10^{19} s^{-1}. In a reactor with zero temperature coefficient a fission rate peak can reach a maximum of 1×10^{21} s^{-1} (Fig. 2). Since such a fission rate fluctuation would be about 100 times the time average fission power, the centre of the kernel will be 164 °C hotter than its surface. In a real fuel this would not be favourable for the integrity of the particle. The temperature difference at the surface of the particle would then be 47 °C.

3.3. Power oscillations

It can be seen, for example from an examination of the peaks in Fig. 5 compared with Fig. 6 and in Fig. 15 compared with Fig. 16, that each peak in the hottest temperature occurs up to a second after a peak in fission power. In most cases the delay is much shorter. Particles are heated during the fission peak. The gas surrounding a particle is rapidly heated as shown in the example in Section 3.1 and expands. In a simplified model of the momentum transfer between expanding gas and a single particle the acceleration and displacement of the particle can be estimated within the time scale of the duration of a peak in fission power. This is an at-

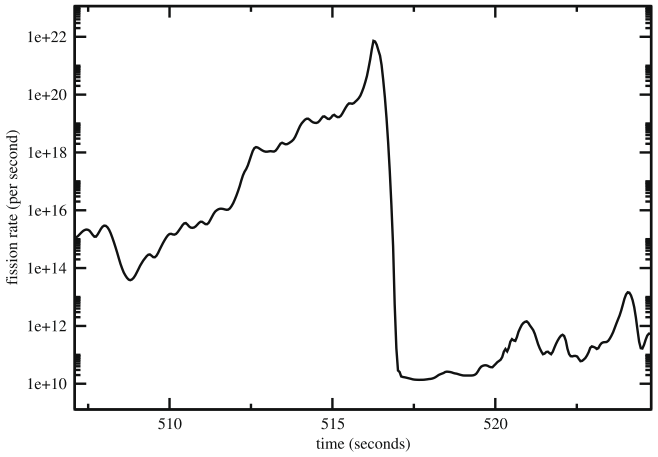

Fig. 15. Fluidized bed reactor with 8% recycled WG plutonium 92% depleted uranium, with hypothetical zero delayed neutron yield and zero temperature coefficient – development of fission power over 36 s around a fission peak at 516.3 s.

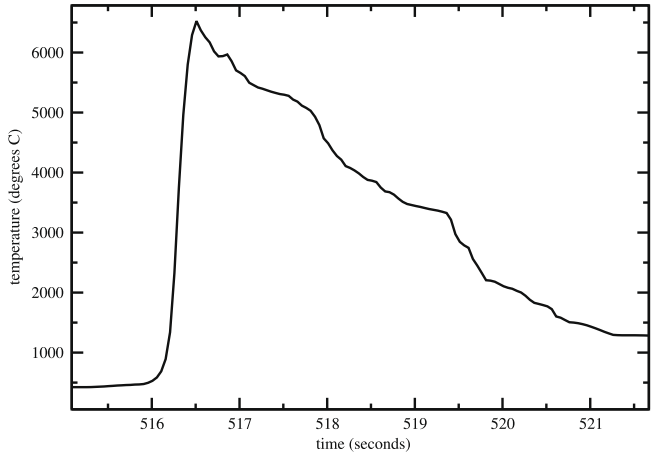

Fig. 16. Fluidized bed reactor with 8% recycled WG plutonium 92% depleted uranium, with hypothetical zero delayed neutron yield and zero temperature coefficient – maximum temperature development with time around a peak temperature at 516.5 s.

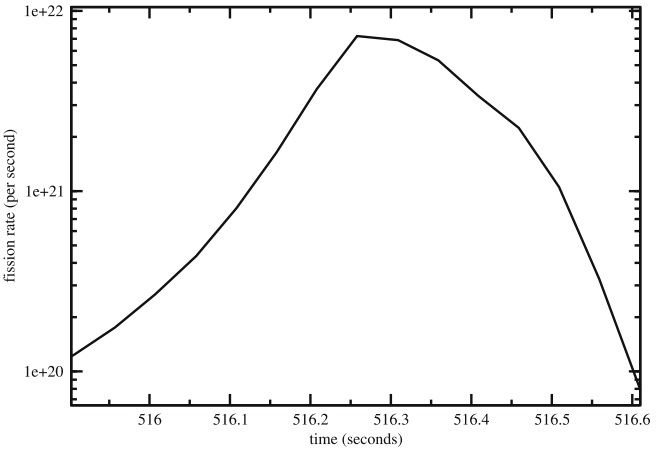

Fig. 17. Fluidized bed reactor with 8% recycled WG plutonium 92% depleted uranium, with hypothetical zero delayed neutron yield and zero coefficient – fission peak over 1 s.

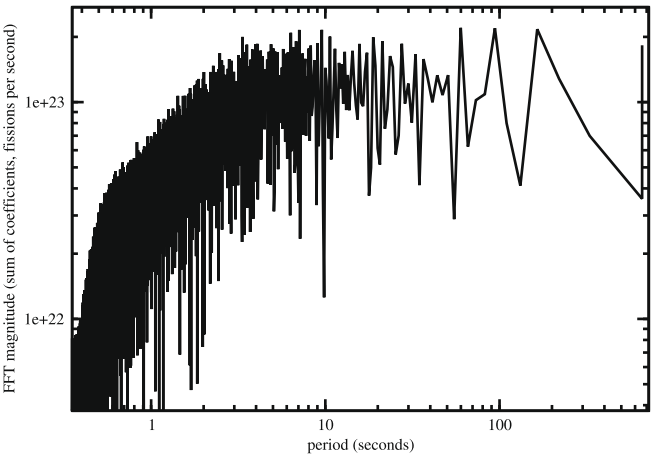

Fig. 18. Fluidized bed reactor with 8% WG MOX, with hypothetical zero temperature coefficient – period analysis of fission rate – Fast Fourier Transform from 2^{15} measured time values (magnitude of the sums of coefficients).

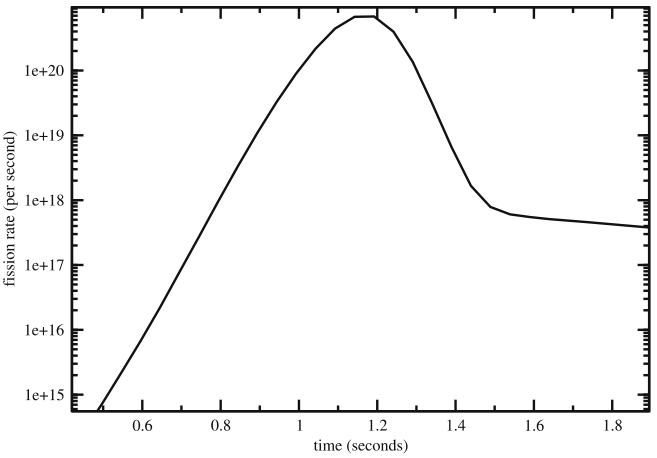

Fig. 19. Fluidised bed reactor with 30% recycled LWR plutonium 70% depleted uranium – initial fission power peak ($1.10^{19} \equiv 320$ MW).

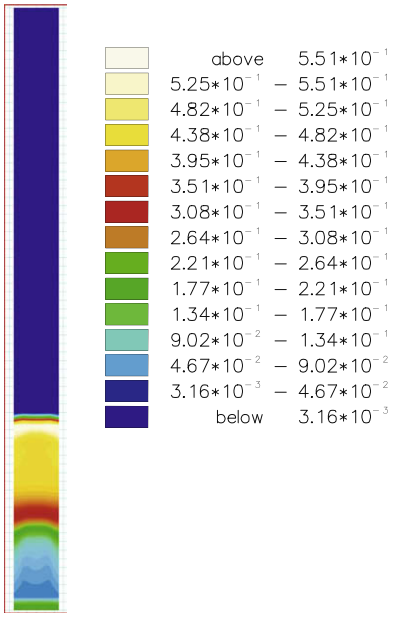

(a) The solid fraction at one second shows a flat slug at the bottom of the reactor.

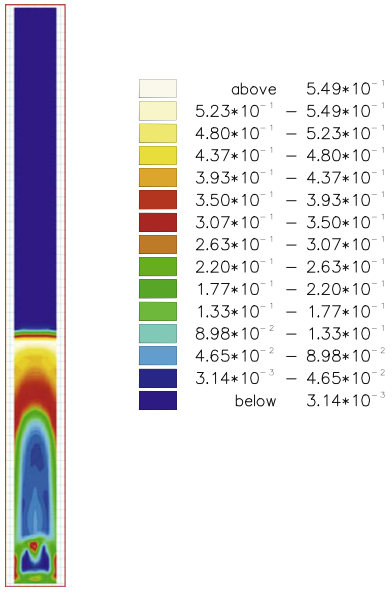

(b) The solid fraction at two seconds shows the first flat slug has risen in the reactor and is beginning to develop into an axial slug. A second slug has appeared at the bottom of the reactor.

Fig. 20. Fluidized bed reactor with 8% recycled WG plutonium 92% depleted uranium, with hypothetical zero temperature coefficient, in a fuel bed extending from 2.5 m radius to 3.5 m, height 13 m – solid fraction at 1 s and 2 s.

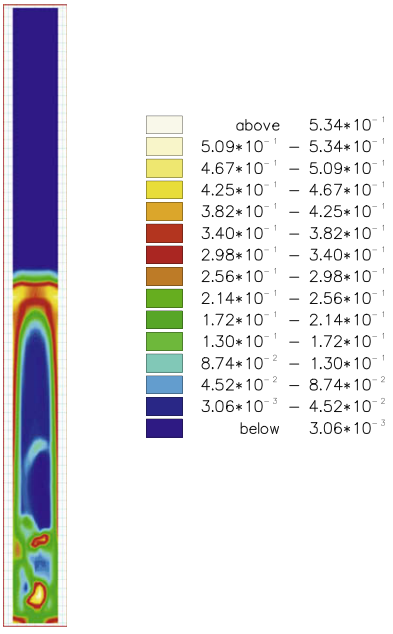

(a) The solid fraction at three seconds shows both slugs have risen further in the reactor. There is a region where the solid fraction is about 0.5, at about half of the height of the reactor cavity.

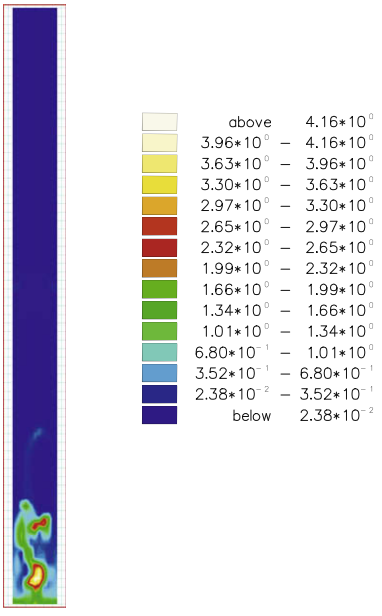

(b)Fission at three seconds extends to 3m height above th efloor of the reactor cavity, indicated by the concentration of shortest time delayed neutron precursors.

Fig. 21. Fluidized bed reactor with 8% recycled WG plutonium 92% depleted uranium, with hypothetical zero temperature coefficient, in a fuel bed extending from 2.5 m radius to 3.5 m, height 13 m – solid fraction and fission at 3 s.

tempt to quantify the possible stability feedback by dispersal of the mass of particles undergoing a neutron chain reaction.

An example is shown in Fig. 6 where solid and gas phase temperatures rise from 1000 °C to 1600 °C in 0.2 s. In a real fuel it would be doubtful whether a particle would survive this transient. Particles disperse as they accelerate rapidly, with a radial acceleration of about 2 m s^{-2} to a radial component of solid velocity of about 1 m s^{-1} after 0.5 s, when the gas radial velocity is 2 m s^{-1}. The development of fission power shown in Fig. 5 is only about a factor of 7 in the same time interval, from 2×10^{20} at 558.3 s to 1.4×10^{21} at 558.8 s.

The relative importance of the feedback mechanisms can be judged from the behaviour of the reactor when the relevant fuel properties are hypothetically removed. Figs. 5 and 6 illustrate the effect of removal of a negative reactivity temperature coefficient.

When the temperature coefficient of reactivity is set to zero the highest peak temperature in Fig. 3 is 2339 °C. When the delayed neutron yield is set to zero (Fig. 12) it is 1761 °C. The doubling time of the fission rate in the approach to this peak is 0.07 s. It should be noted that a calculation with no delayed neutron yield never represents a real fuel. It is a tool for investigation of stability.

When both these fuel properties are set to zero (Figs. 13 and 14) the highest peak temperature in this unreal fuel would be 6525 °C, a temperature much greater than would be tolerable in practice. Although the peak fission rate is reached in several stages (Fig. 15), the temperature rise is continuous and rapid (Fig. 16 unlike Fig. 10). The subsequent cooling of the fuel bed is determined by its mass and specific heat. The doubling time of the heat input from fission in the approach to the peak is 0.05 s (Fig. 17). This response is quicker than that when only the reactivity coefficient is made zero. Perhaps more important is the more gradual build up of fission power in the previous 7 s from 508 s to 515 s shown in Fig. 15.

The power spectrum can be examined for evidence of possible periodicity of the fission peaks. A Fast Fourier Transform (FFT) of 2^{15} fission power measurements in the WG MOX reactor, with hypothetical zero reactivity temperature coefficient (Fig. 18) shows a range of larger Fourier coefficients around a period of 3–10 s and again 60–200 s but no period is dominant. This compares with the fission peaks spaced at about 200 s in Fig. 4.

3.4. Initial conditions and first peak in fission power

The initial coolant flow is instantaneously the same value as at full power. The bed starts already partly expanded, with uniform distribution of the solid phase. The iteration process described in Miles et al. (submitted for publication), to determine the reactor geometry for a time dependent calculation, can result in different initial conditions and different time dependent behaviours over the following few seconds. With a typical MOX fuel (ex LWR Pu) there is an early fission rate peak, after 1.2 s. This is shown in detail in Fig. 19. The chosen temperature at time zero is 727 °C. The local temperature, where a prompt critical response has occurred, rises to a peak of 1171 °C after 1.4 s.

The doubling time of the fission rate in the approach to the fission peak in Fig. 19 indicates a characteristic reactor response time of approximately 0.05 s. (That is an increase in the neutron population due to fission by a factor exp(1), see Stacey, 2004[23, Example 5.3].) Such a reactor period would imply a surplus prompt reactivity, derived from Duderstadt and Hamilton (1976, Fig. 6-3) of one dollar. This can be compared with the much greater prompt surplus reactivity at 0 s, 0.0065, as determined in a static calculation with the same material constants and geometry.

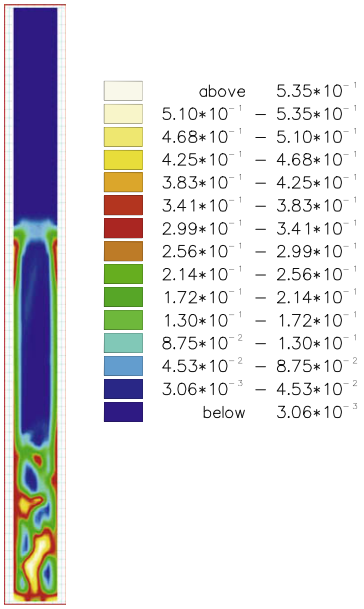

(a) The solid fraction at four seconds shows the top of the first slug has risen about two thirds of the height of the reactor cavity and is beginning to break through the upper surface of the bed. Bubbles replace slugs at the bottom of the reactor.

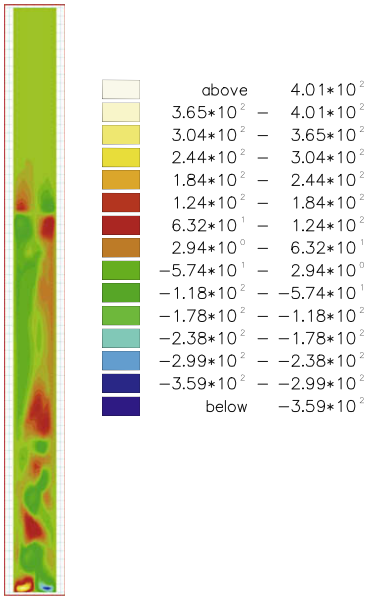

(b) Radial component of solid phase velocity (cm/s) at 4 seconds. Evidence of eddies can be seen where downwards recirculation of particles causes the greatest velocity gradients.

Fig. 22. Fluidized bed reactor with 8% recycled WG plutonium 92% depleted uranium, with hypothetical zero temperature coefficient, in a fuel bed extending from 2.5 m radius to 3.5 m, height 13 m – solid fraction and radial component of velocity at 4 s.

In ^{239}Pu, usually the dominant fissile isotope, the delayed neutron fraction is 0.0022 and in ^{241}Pu it is 0.0054. The delayed neutrons from MOX fuel are largely from ^{239}Pu. When they are taken in account, the total positive step reactivity insertion is approximately 0.009. The reduction in fission rate after 1.2 s shows the time scale of the non-uniform redistribution of the particles in the fluidized bed. In comparison the initial prompt surplus reactivity with LEU fuel is much greater, +0.019 according to a static calculation. In spite of the greater surplus reactivity the first peak occurs only after 48 s (Fig. 3). This must be explained by the greater negative temperature coefficient of a fuel with fissile uranium compared with one containing fissile plutonium.

The behaviour of a reactor during the first few seconds can be examined with the aid of frequent snapshots. The initial transient behaviour has been examined in this way for a fuel which is hypothetical, with zero temperature reactivity coefficient. The choice of initial temperature has in this case no effect on reactivity. In fact an elevated temperature is chosen in order to save computer time. A cold bed would require minutes to be heated to operating temperature by the average fission heat. It is initially expanded to 2.9 m, compared with a packed height of 2.1 m. At this expansion the eigen value is 0.987. In a time dependent calculation a typical expansion after 300 s, up to 1200 s, is between 5 m and 9 m. In a uniformly expanded bed the Eigen value increases with expansion. If these were really uniform expansions to 5 m or 9 m the eigen values would be approximately 1.05 or 1.09. The change in solid distribution during the first 5 s is shown, once per second, in Figs. 20, 21a, 22a and 23a.

The side reflector and the core extend to 5 m above the bottom of the cavity. Fission might be expected to take place up to the top of the reflector. In fact, as indicated by the delayed neutron precursors (see Fig. 21b), it extends only to 3 m height, even when the bed has expanded beyond the height of the reflector. At 1 s the spatial distribution of the delayed neutron precursors in all delayed groups resembles the fast flux distribution in a static calculation. Later, after 3 s (Fig. 21b) and after 5 s (Fig. 23b), it is limited by the changed distribution of the solid phase. At 3 s there is still no difference between the spatial distribution of the precursors in the six delayed groups. At 5 s the short term precursors extend to 3 m (see Fig. 23b) but the long term precursors extend from 2.5 m to 6 m (see Fig. 24), indicating how the particles undergoing fission in the first 3 s have travelled in the following 2 s. This spatial distribution of the long term precursors can be compared with that of the solid in general, Fig. 23a. At most times these spatial distributions would be identical, but not at start up. The particles which have recirculated down into the lowest part of the cavity (the solid phase from cavity floor to a height of 2.5 m) have only started to undergo fission. The solid phase distribution after 1 s shows a flat slug which has developed in the lower part of the reactor. This slug breaks through the top of the bed at 4 s. Meanwhile a second slug develops below it, which breaks up into bubbles before it reaches the top of the bed. The top of the bed reaches two-thirds of the height of the reactor at 4 s and falls back to about one-third of the height at 5 s, when the slugs have all been replaced by bubbles. The fuel cavity is 14 m tall. At all times the exit gas contains no more than the contour value of 0.0032 solids. A detector at gas exit records a value briefly up to 2×10^{-4} at the inner wall during the first fission peak and less than 2×10^{-9}, in the centre or at the outer wall, during peaks thereafter.

A long term calculation with the same fuel shows that the first fission peak is not until 356 s. Contour plots are available at 20 s intervals. A plot of solid fraction at 340 s shows a bed which is ex-

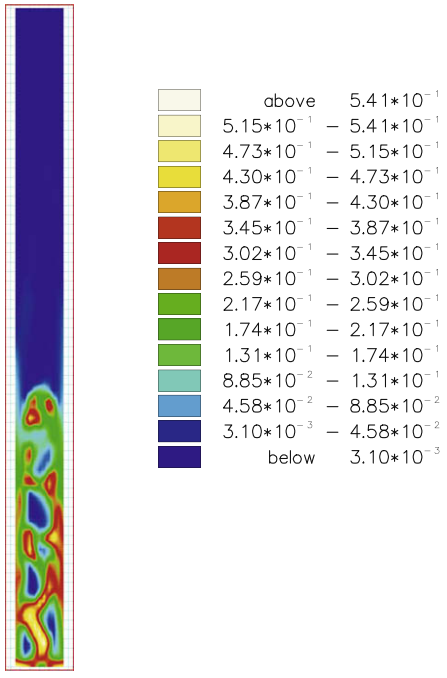

(a) The solid fraction at five seconds shows that large bubbles have replaced slugs in the lower part of the bed. The upper surface of the bed has fallen to about one third of the height of the reactor.

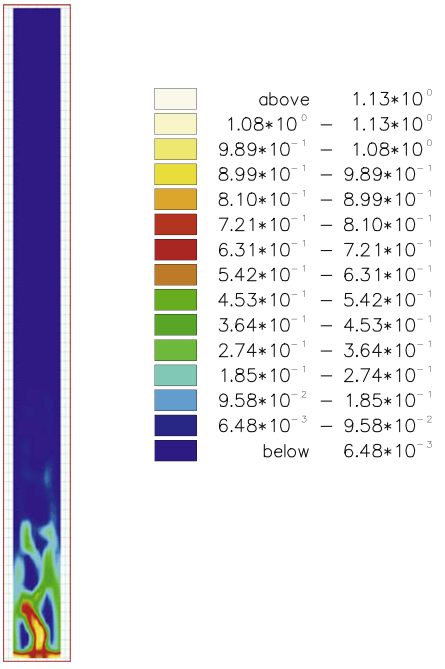

(b) Fission at five seconds extends to 3m height above the floor o fthe reactor cavity, indicated by the concentration of delayed neutron precursors, shortest time delayed group.

Fig. 23. Fluidized bed reactor with 8% recycled WG plutonium 92% depleted uranium, with hypothetical zero temperature coefficient, in a fuel bed extending from 2.5 m radius to 3.5 m, height 13 m – solid fraction and fission at 5 s.

panded up to 5 m, with small bubbles. At 360 s the solid fraction again reaches 5 m but with large bubbles. This is some evidence to support the hypothesis that smaller bubble size results in greater reactivity and that a subsequent generation of heat by greater nuclear fission reaction produces larger bubbles or slugs in the fluidized bed, reducing reactivity.

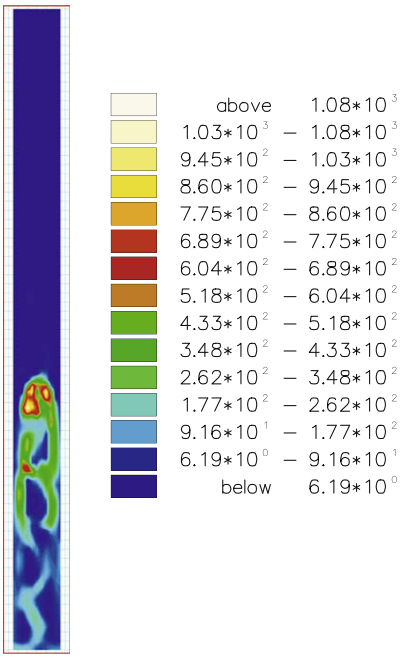

Fig. 24. Fluidized bed reactor with 8% recycled WG plutonium 92% depleted uranium, with hypothetical zero temperature coefficient, in a fuel bed extending from 2.5 m radius to 3.5 m, height 13 m. Concentration of delayed neutron precursors, longest time group, at 5 s extends from 2.5 m to 6 m.

Recirculation of solids is shown by Fig. 25a, the axial component of solid phase velocity. A greatest downward velocity can be seen against both walls from about 5 m down. This can even be seen in the axial component of the gas phase velocity (Fig. 25b), where gas against the same walls is dragged downwards by falling solid phase. Solids in the uppermost 6 m of cavity have at this instant in time a smaller downwards velocity, zero at the upper boundary of the cavity. The greatest upwards velocity of both phases is at mid height of the cavity, away from the walls. The radial component of solid phase velocity (Fig. 22b) indicates eddies at locations where the gradients of the axial component are greatest.

4. Summary and conclusions

Stability of a nuclear reactor with respect to short term fluctuations of power level depends on reactivity variation with temperature. Stability feedback associated with a change in fuel temperature in a reactor takes place essentially instantaneously. A significant part of prompt feedback usually comes from the change in resonance escape probability due to Doppler broadening of resonances. The moderator may also contribute a reactivity temperature coefficient by changes in its scattering and thermalisation of neutrons. The change in reactivity with temperature may not be in the desired direction, especially with plutonium fuel. Depending on fuel composition, for example as it changes with burn up, and on the proportion of fuel and moderator in a pebble, it is possible for a positive coefficient to occur. An additional means of removing

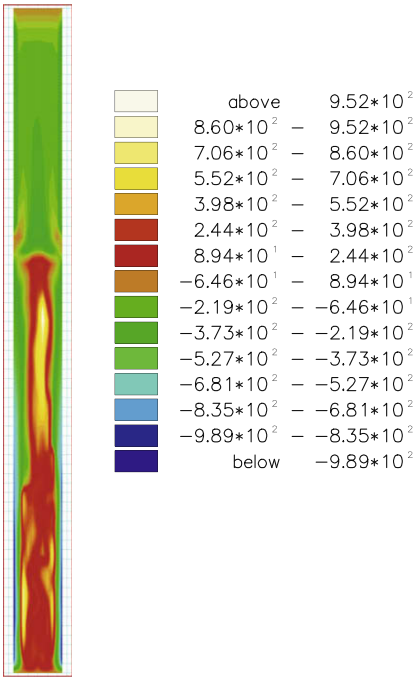

(a) Axial component of solid phase velocity (cm/s) at 4 seconds. Downwards recirculation of particles at the walls of the lower part of the cavity.

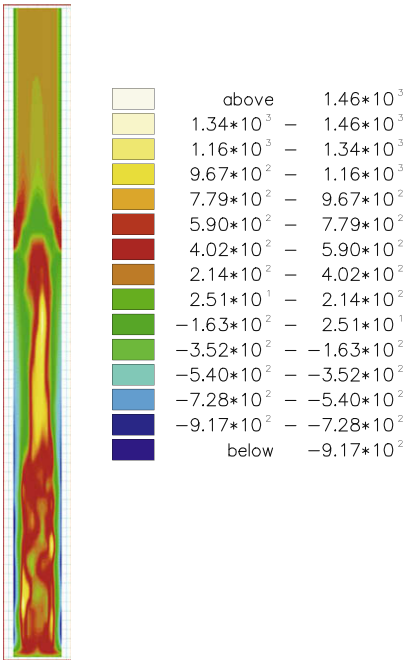

(b) Axial component of gas phase velocity (cm/s) at 4 seconds. Downwards recirculation of gas at the walls of the lower part of the cavity.

Fig. 25. Fluidized bed reactor with 8% recycled WG plutonium 92% depleted uranium, with hypothetical zero temperature coefficient, in a fuel bed extending from 2.5 m radius to 3.5 m, height 13 m – axial components of velocities at 4 s.

excess reactivity would offer the possibility of using fissile material with a positive temperature coefficient.

The fluidized bed reactor may have this additional means of stability feedback. It is important to understand in some detail the feedback mechanisms in this reactor. They are investigated individually in time dependent calculations using hypothetical fuels with

- no temperature coefficient of reactivity (no Doppler broadening),
- no delayed neutrons,
- neither temperature coefficient nor delayed neutrons.

The real fuel which is used as a basis for these investigations is MOX with 8% WG plutonium. Compared with other MOX fuels this has the smallest delayed neutron fraction, since ^{239}Pu has a smaller delayed neutron fraction than ^{241}Pu.

Major fission rate peaks are accompanied by peaks of temperature. A reduction to zero of the fraction of neutrons which is delayed increases peak temperatures. The period between temperature peaks remains unchanged compared with that of the real fuel, between 30 s and 60 s. The amplitudes of the fluctuations between minimum and maximum temperature increase.

A negative coefficient of reactivity with temperature aids short term stability. Without it the fluctuations in fission rate and temperature are greater. The period between temperature peaks increases greatly, to between 120 s and 200 s. They remain still stable. Maximum temperature increases while mean fission power decreases.

When both of these mechanisms are set to zero the maximum temperature becomes much greater than would be tolerable in practice. However the calculations show that the reactor does not become unstable. This large, rapid increase in temperature is caused by an increase of fission rate in stages over a period of about 10 s. The fluctuations in temperature become greater. The time intervals between peak values are between 80 s and 180 s.

One stability feedback mechanism is sufficient. On the other hand each additional mechanism increases stability and therefore the available fission power within the limits of the reactor construction materials and its fuel.

When the temperature reactivity coefficient is not zero, it is the obvious link between bed thermal inertia, long term temperature period and reactivity. Otherwise the link is probably the effect of temperature on bubble size and therefore on the chance of favourable geometry occurring in the fuel bed (thermal utilization, resonance escape probability and neutron escape). The short term period of temperature fluctuation is caused by bubble movement in a region where fission is taking place, especially when the bubble size is large.

The behaviour of the fluidized bed reactor just after start up has been investigated in some detail. During the first few seconds after the start of gas flow the type of fluidization changes. Initially a flat slug begins to move up from the bottom of the fuel bed. The slug becomes axial and recirculation of solids begins at 4 s. In plutonium fuels the initial peak is very sensitive to the initial reactivity.

Further investigation of the behaviour of the reactor just before, during and after a major peak in fission rate should provide more insight into stability feedback.

References

Alander, A. et al., 2006. From once-through nuclear fuel cycle to accelerator-driven transmutation. Nuclear Physics A 562, 630–633.

Cuevas Vivas, G.F. et al., 2002. Optimisation of MOX enrichment distributions in typical LWR assemblies using a simplex method-based algorithm. Annals of Nuclear Energy 29, 2001–2017.

Duderstadt, J.J., Hamilton, L.J., 1976. Nuclear Reactor Analysis. John Wiley and Sons, New York.

Fetterman, R., 2009. AP1000 core design with 50% MOX loading. Annals of Nuclear Energy 36, 324–330.

Franceschini, F., Petrovic, B., 2008. Core physics analysis of 100% MOX core in IRIS. Annals of Nuclear Energy 35, 1587–1597.

Francois, J.L. et al., 2002. Design of an overmoderated fuel and a full MOX core for plutonium consumption in boiling water reactors. Annals of Nuclear Energy 29, 1953–1965.

Frois, B., 2008. Nuclear energy in a global context. Nuclear Physics A 805, 320c–327c.

Galperin, A., 1995. Utilization of light water reactors for plutonium incineration. Annals of Nuclear Energy 22, 507–511.

Glasstone, S., 1967. Sourcebook on Atomic Energy. Van Nostrand Reinhold, New York.

Hetrick, D.L., 1993. Dynamics of Nuclear Reactors. American Nuclear Society, La Grange Park, Illinois.

Hoggett-Jones, C. et al., 2002. Modelling the inventory and impact assessment of partitioning and transmutation approaches to spent nuclear fuel management. Annals of Nuclear Energy 39, 491–508.

Jo, C.K. et al., 2000. Graphite-filled mixed-oxide fuel design for fully loaded PWR cores. Annals of Nuclear Energy 27, 819–829.

Kuijper, J.C. et al., 2006. HTGR reactor physics and fuel cycle studies. Nuclear Engineering and Design 236, 615–634.

Lombardi, C., Mazzola, A., 1996. Exploiting the plutonium stockpiles in PWR's by using inert matrix fuel. Annals of Nuclear Energy 23, 1117–1126.

Masson, M. et al., 2006. Block-type HTGR spent fuel processing: CEA investigation program and initial results. Nuclear Engineering and Design 236, 516–525.

Miles, B.E. et al., 2010. Simulation of a gas-cooled fluidized bed nuclear reactor. Part 1: Mixed oxide fuels. Annals of Nuclear Energy 37, 999–1013.

NEA/OECD, 2006. French R and D on the Partitioning and Transmutation of Long-lived Radionuclides. An International Peer Review of the 2005 CEA Report, Number 6210.

Pain, C.C. et al., 2002. Space-dependent kinetics simulation of a gas-cooled fluidized bed nuclear reactor. Nuclear Engineering and Design 219, 225–245.

Pain, C.C. et al., 2003. An investigation of power stabilisation and space-dependent dynamics of a nuclear fluidized-bed reactor. Nuclear Science and Engineering 144, 242–257.

Paratte, J.M., Chawla, R., 1995. On the physics feasibility of LWR plutonium fuels without uranium. Annals of Nuclear Energy 22, 471–481.

Rots, P.E.A., van der Hagen, T.H.J.J., 1996. Fluidized bed nuclear fission reactor. Chemical Engineering Science 51 (11), 2763–2768.

Salvatores, M., 2006. Fuel cycle strategies for the sustainable development of nuclear energy: the role of accelerator driven systems. Nuclear Physics A 562, 578–584.

Stacey, Weston M., 2004. Nuclear Reactor Physics. Wiley-VCH Verlag, Weinheim, Germany.

Thilagam, L. et al., 2009. A VVER-1000 LEU and MOX assembly computational benchmark analysis using the lattice burnup code EXCEL. Annals of Nuclear Energy 36, 505–519.